https://doi.org/10.20965/jrm.2024.p0229

Paper:

Development and Validation of an Instrument for Wave Height Measurement with Encoder Sensors and Accelerometer

Devit Suwardiyanto*, Endi Sailul Haq*, Mohamad Dimyati Ayatullah*, and Bayu Rudiyanto**

*Politeknik Negeri Banyuwangi
Jl. Raya Jember KM 13, Kabat, Banyuwangi, East Java 68461, Indonesia
E-mail: endi@poliwangi.ac.id
**Politeknik Negeri Jember
Jl. Mastrip No.164, Jember, East Java 68121, Indonesia
[Received July 6, 2023; accepted October 23, 2023]

Ocean waves play a significant role in coastal dynamics and the management of coastal development activities. However, there are limited instruments to measure the wave height, particularly in developing countries. This study introduces a novel instrument design for simple and cost-effective wave height measurement. The proposed instrument combines a Hall-effect sensor and an accelerometer to capture the rise and fall of a buoy in response to wave movements. The Hall-effect sensor as a rotary encoder detects the rotation of the buoy while the accelerometer measures the tilt of the instrument caused by ocean waves. The instrument is constructed using PVC pipes and incorporates long-range (LoRa) communication technology for real-time monitoring. Experimental tests were conducted at a study site in Banyuwangi Regency, Indonesia, where the performance of the instrument was compared with an ultrasonic sensor-based instrument. The results validate the effectiveness of the proposed instrument design for wave height measurement. The collected data were transmitted via the LoRa communication system, enabling convenient monitoring and analysis of sea-level changes. The valuable contribution of the instrument to the field stems from its precision in measuring the wave height, adaptability to diverse conditions, and potential applicability in shallow waters.

Keywords: ocean waves, wave height measurement, encoder, accelerometer, Hall-effect sensor

1. Introduction

Ocean waves are the rising and falling movements of seawater perpendicular to sea level that form sinusoidal curves [1]. These waves arise because of the disturbing force that occurs in free bodies of water. Ocean waves can be classified into several types based on their generating force: (1) wind waves; (2) tidal waves, which are caused by the gravitational pull of the sun and moon; and (3) tsunamis, which are generated by earthquakes [2]. During the tsunami at Sunda Strait at the end of 2018, large ocean waves were generated from landslides of Mount Anak Krakatau [3].

Wave height is a crucial parameter that should be regularly measured in Indonesia and other maritime countries because it can influence coastal dynamics. However, instruments that can be used to monitor wave height are limited [4], even though developed countries such as China and some European countries have long developed and utilized the available instruments [5]. Wave data can help in managing and arranging coastal development activities, such as ports or tourism [6] and shipping lanes [7], as well as in detecting climate change [6] and hazards that threaten the safety of fishermen and nearby communities [3].

Ocean waves occur abruptly, randomly, and dynamically, making them difficult to predict, calculate, and formulate mathematically [8]. Fortunately, studies have been conducted on the measurement and monitoring of wave heights using a variety of instruments and methods. Most available instruments utilize buoys placed at a predetermined point in seawater and are equipped with several devices to record information related to wave changes. Buoys are equipped with GPS signal receivers detected by satellites to measure the wave height by calculating the position of the buoy and eliminating unwanted rotational motion. The use of GPS has been proven to provide more reliable data because it has no moving parts compared with a conventional accelerometer or gyroscope buoy [9]. Neural network algorithms were applied to remove noise, and a Gaussian low-pass filter was used to obtain an appropriate wave spectrum [10].

In addition to adopting GPS in the instruments, other studies also added motion sensors and a microcontroller called spotter [11]. Wave measurements were performed using image processing to measure the distance between the first and latest positions of the buoy using the recorded coordinates. Devices may utilize accelerometer, gyroscope, and magnetometer sensors to measure the wave height because these sensors are relatively low cost and small. These sensors are easier to place on a buoy, require low DC voltages, are directly connected to a microcontroller, and provide consistent ocean wave readings [4, 6, 7, 12–14].

The wave height is generally measured using instru-

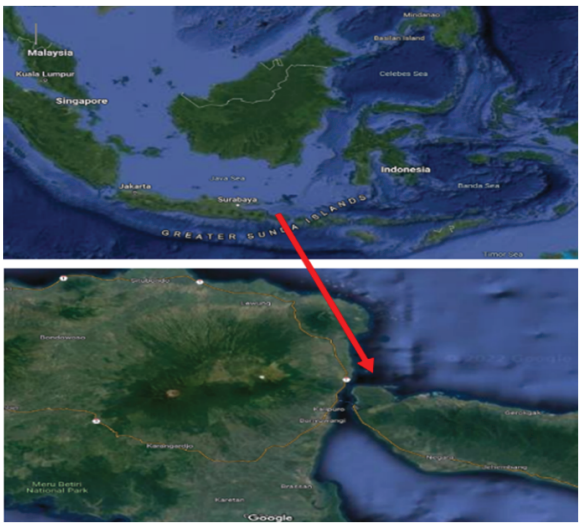

Fig. 1. Field deployment location.

ments that exploit buoys, altimeter sensors [15], LIDAR sensors [16, 17], pressure sensors [18], ultrasonic sensors attached to drones [19], and smartphone sensors [20]. Among all the available sensors, ultrasonic sensors are favored because they are relatively inexpensive and have good wave height measurement results; however, this sensor is difficult to use in deep water because it requires a stable position.

This research aims to develop and validate a novel instrument design for simply measuring wave height. This newly constructed instrument takes advantage of the rise and fall of the buoy using a Hall-effect sensor and an accelerometer. A Hall-effect sensor is a touchless switch or a switch triggered by a magnetic field. This sensor was used to read the rotation of wave height changes. The working principle of this sensor is to reduce the negative effects of seawater that can cause tool corrosion. An accelerometer sensor was used to read the slope of the tool due to currents and ocean waves. This study was conducted to address the scarcity of marine monitoring instruments in Indonesia owing to their high price and maintenance costs. Therefore, the proposed instrument was built at a low cost using a PVC pipe and long-range (LoRa) communication device. We also adopted the "Internet of Things" concept to facilitate real-time sea-level monitoring more easily.

2. Material and Methods

2.1. Test Location

The study site was located at 8°04′15.9″S 114°28′44.8″E in Banyuwangi Regency, East Java, Indonesia, on November 19–23, 2020 (**Fig. 1**). The instrument was placed in the sea at a certain depth based on the distance between the LoRa device and the shoreline. The study site had relatively calm sea waves with wave heights significantly below 2 m, which was suitable for testing the instrument.

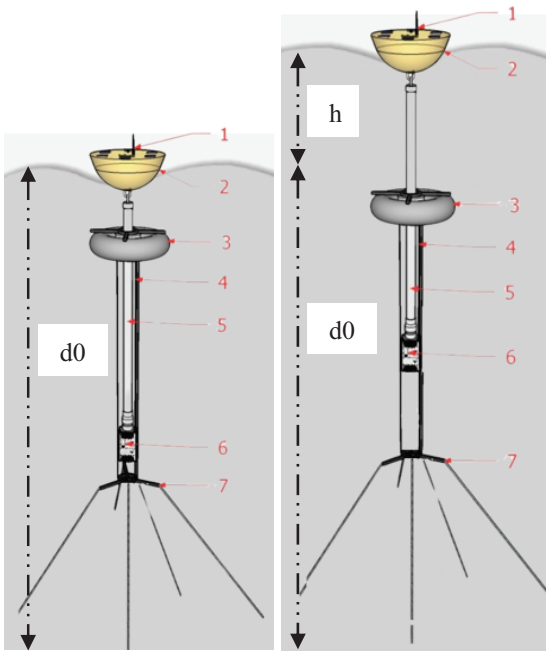

Fig. 2. Simulation of sensor responses to wave height (1. communication devices; 2. buoy; 3. subsurface buoy; 4. timing belt; 5. outer and inner PVC pipes; 6. sensor block; 7. anchor).

The wave sensor constructed in this study was developed from a previous study, which has several drawbacks: (1) it is unsuitable for placement in deep water, and (2) there is a high possibility of corrosion of its column due to seawater. Therefore, this study was conducted to improve upon this and mainly focused on measurement aspects, such as wave height and seawater changes acting upon the encoder sensors and accelerometer design. The previously built instrument was improved by upgrading its material, sensor, and pipe to deeper water, as shown in **Fig. 2**.

2.2. Sensor

The sensor body in **Fig. 2** comprises two main parts:

1) The buoy is designed to follow the movement of water particles on the surface of the sea so that it can detect movement. The shape of the buoy is shown in the following image. The materials used for the buoy were a mixture of resin and matt (fiber), with a diameter of 100 cm and a height of 50 cm.

2) The pipe in **Fig. 3** and the sensor recorded sea-level changes. The pipe was constructed using PVC pipes, which consisted of an outer pipe (diameter: 6 inches; length: 5 m) and an inner pipe (diameter: 3 inches; length: 5.5 m). The outer pipe was connected to a rope attached to an anchor at five fixed points (multipoint mooring system), whereas the top part was connected to a subsurface buoy that kept the outer pipe upright. The inner pipe was connected to a fiber buoy (diameter: 100 cm; height: 50 cm).

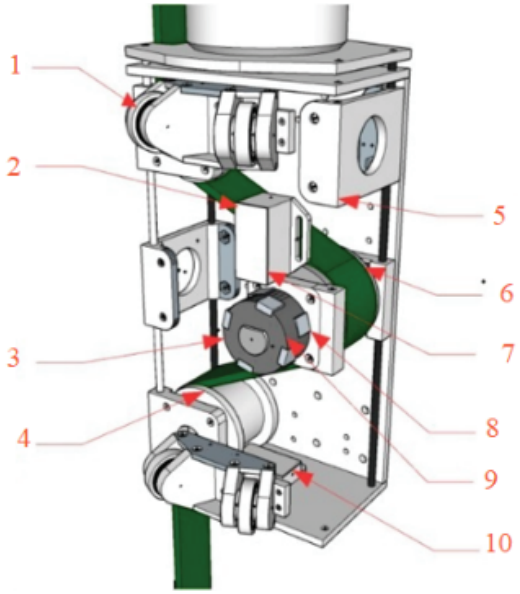

Fig. 3. Sensor block design (1. free wheel; 2. timing belt; 3. shaft; 4, 6. gear; 5. body holder; 7. Hall-effect sensor; 8, 9. magnets; 10. accelerometer).

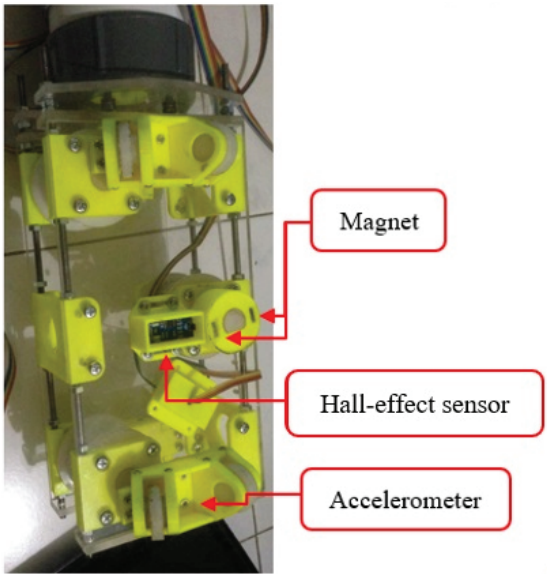

Fig. 4. Sensor block constructed using PVC pipes.

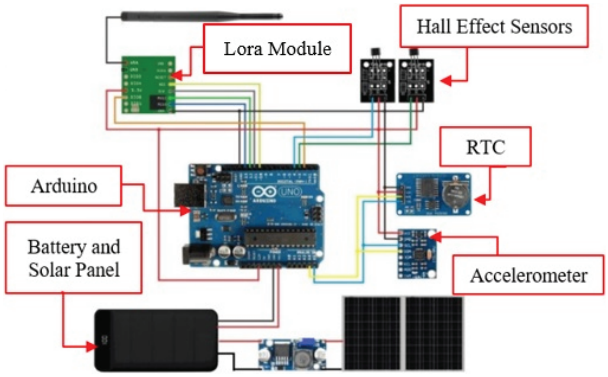

Fig. 5. Configuration of components and power supply.

The sensor block shown in **Fig. 3** consists of two components: an encoder sensor that utilizes a Hall-effect sensor and an accelerometer. Hall sensors are used to measure the position of the magnetic pole of the rotating plastic gear. They were installed to detect vertical buoy movement. Wave height information was obtained by demodulating the magnetic field value. This study utilized five linear Hall sensors as magnetic pole position detection components, specifically the A3144 Hall-effect sensor produced by MXRS [21].

A Hall-effect sensor is an electronic component that can detect magnetic fields and react accordingly to variations in the field intensity. It converts magnetic or magnetically encoded information into electrical signals, which can then be processed using electronic circuits. The Hall element serves as a fundamental magnetic field sensor. Signal conditioning is necessary to ensure that the output is suitable for most applications [22–25].

The potential difference between the two electrodes was 0 V when the magnetic field was unaffected, indicating no current flow between the two electrodes. However, in the presence of a magnetic field, it produces current flows that move closer to or further away from the side affected by the magnetic field. This resulted in a potential difference between the two electrodes of the Hall-effect sensor, which was equal to the magnetic intensity received by the Hall-effect sensor.

The encoder sensor was connected to a timing belt placed on the outer pipe. This is important because the buoy movement pulls or pushes the inner pipe, which allows the encoder sensor to rotate freely following the buoy movement. An accelerometer sensor was used to record changes in the pipe tilt caused by ocean waves. To investigate the use of an accelerometer for motion monitoring in an unrestrained environment, an experimental study was conducted, as shown in **Fig. 4**. An accelerometer has also been used to measure the motion of the human body in various situations, such as walking, running, and jumping [26]. This recorded angle of inclination was then converted using trigonometric equations to obtain the change in the wave height perpendicular to the initial position.

A real-time clock (RTC) device was used to record wave height readings in real time. All recorded data were sent through the LoRa HopeRF at 433 MHz radiofrequency. An Arduino Uno microcontroller was used to read and transmit data every 100 ms to a gateway located on the land. The gateway was built using an ESP32 connected to a LoRa HopeRF with the same frequency. ESP32 was chosen because it can easily connect to a hotspot and the Internet. The data received by the ESP32 were sent to the database by adopting IoT using the MQTT protocol.

The power source required to supply all the devices was a 2×10 WP solar cell placed on top of the buoy at a 20° angle to capture optimal sunlight. The solar cell was connected to a voltage stabilizer and a 12 V battery was placed inside the buoy, as shown in **Fig. 5**.

2.3. Mechanism of Wave Height Measurement

Wave height measurements were conducted by simply utilizing the vertical movement of the buoy due to changes in sea level. The buoy movement pulled both pipes, and the gear on the encoder rotated as it was connected to the timing belt. The encoder detected each rotation and converted it into a distance value using a Hall-effect sensor [27].

Constructed using polactic acid and acrylic materials, this instrument was designed to facilitate vertical movement such that the diameter adjusts to the outer pipe. At each corner point, eight free wheels made of Teflon were installed to reduce the friction with the outer pipe when moving up and down. To maintain the Hall-effect sensor while properly reading the movement, the timing belt should not be shifted or loosely installed on the instrument. Therefore, three gear holders were created, in which one gear shaft was connected to two magnets. An accelerometer was installed at the bottom to measure the instrument tilt.

To construct an instrument that can properly record wave height, the buoy design shown in **Fig. 6** should be applied, where the force of the buoy must be greater than the weight of the deepest pipe. This design is assumed to support the pipe in floating and flexibly following the water movement. According to the buoyancy law, the above model can be calculated using Eqs. (1) and (2):

$$F_{B1,2} = V_{Buoy}\rho_f g, \quad \ldots\ldots\ldots\ldots \quad (1)$$

$$F_{g1,2} = (W_{Buoy} + W_{iPVC})g. \quad \ldots\ldots\ldots \quad (2)$$

where

F_{B1}, F_{B2}: Buoyant force [N]
V_{Buoy}: Displaced body volume of liquid [m^3]
ρ_f: Fluid density [kg/m^3]
F_{g1}, F_{g2}: Weight force [N]
W_{Buoy}: Weight of the buoy [kg]
W_{iPVC}: Weight of the inner pipe [kg].

To determine the dimensions of the subsurface buoy for it to float perpendicularly on water, the rule should be applied. That is, the buoyant force on the subsurface buoy must exceed the weight of the outer pipe. In this study, the subsurface buoy was composed of tires encircling the top of an outer pipe. The selected study site has ocean waves or currents that are not strong enough to significantly affect the tilt of the floating pipe.

Ocean waves were measured using an encoder sensor to monitor the position changes in the shaft. Four pairs of magnets were arranged around the shaft. Position changes can be used to measure the linear distance by counting the number of pulses compared with the known number of pulses per arc length around the magnetic wheel. The length of the position change (L) of the encoder can be calculated by dividing the number of pulses (P) by the number of pulses per 1 inch arc length (PPI), where PPI generated from pulses per revolution (PPR) divided by the circumference of the magnet gear in the sensor block, where "r" represents the radius of the magnet gear, as shown in Eqs. (3) and (4):

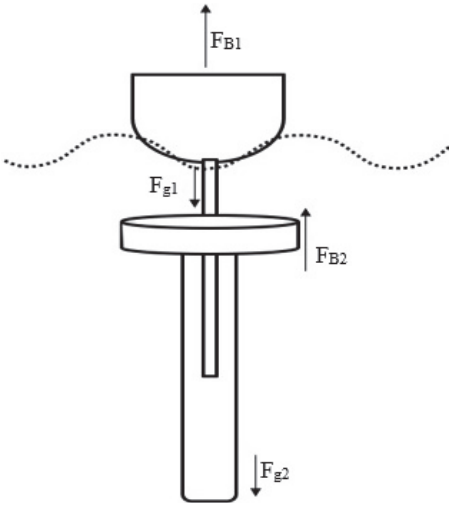

Fig. 6. Subsurface buoy model.

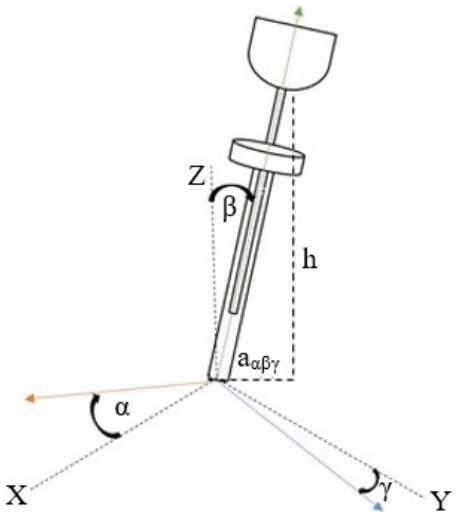

Fig. 7. Tilt angle buoy.

$$PPI = \frac{PPR}{2\pi r}, \quad \ldots\ldots\ldots\ldots \quad (3)$$

$$L = \frac{P}{PPI}. \quad \ldots\ldots\ldots\ldots \quad (4)$$

The rotation direction of the encoder was determined by detecting the square wave signal produced by the two Hall-effect sensors, as shown in **Fig. 5**. The instrument was designed to detect sea wave changes through two channels: A and B. Channel A was ahead of channel B, indicating a drop in sea waves, and vice versa. The distance between the magnets was 2.2 cm.

The three-axis accelerometer sensor [28] was used to calculate the tilt caused by ocean waves and currents, as shown in **Fig. 7**, which detects changes in the tilt angles on the X-, Y-, and Z-axes. The tilt angle obtained from these three angles α, γ, and β as the change of the pipe

Table 1. LoRa configuration.

No.	Settings	Value
1	Bandwidth	500 kHz
2	Coding rate	4/5
3	Spreading factor	128 chips/symbols
4	CRC	On
5	Transmission power	20 dBm

angle is derived from Eq. (5).

$$a_{\alpha\beta\gamma} = \sqrt{\alpha^2 + \gamma^2 + \beta^2}. \quad \ldots\ldots\ldots\ldots \quad (5)$$

Furthermore, the change in the water level (h) can be calculated based on the angle and length of the position changes (L) from Eq. (4).

$$h = \cos a_{\alpha\beta\gamma} \cdot L. \quad \ldots\ldots\ldots\ldots\ldots\ldots \quad (6)$$

Therefore, the changes in sea depth can be determined by adding the reference level sea depth (d_0) to the changes in wave height from Eq. (6), as shown in **Fig. 2**.

$$D = h + d_0. \quad \ldots\ldots\ldots\ldots\ldots\ldots \quad (7)$$

where

h: Wave height [cm]
D: Ocean depth [cm]
d_0: Reference level [cm].

The test scenario was conducted by comparing the measurement results of the novel instrument with those of an ultrasonic instrument. This method was used to verify and validate the measurement results. The obtained data were processed using the Wafo MATLAB Toolbox to determine the characteristics of the water at the test location.

The constructed ultrasonic instrument uses non-contact ultrasonic sensors for water level measurement, which are implemented in a maritime environment [29] and water in a container [30, 31] with a sensitivity of 1 mm. Accordingly, the data read by the ultrasonic sensor were assumed to be actual sea level change data in this study.

2.4. Buoy Communication

The LoRa communication system was designed for easier monitoring of sea level changes [32] and more flexible data storage and processing. The communication system developed in this study consisted of sensor nodes (buoys) and gateways that utilized the HopeRF-RFM9x radio communication module at a frequency of 915 MHz. The module listed in **Table 1** was established using the fastest physical layer settings with the highest transmission power to work efficiently in a short period.

The sensor node sent wave height data and the recorded time in the YY-MM-DD HH-MM-SS format every 100 ms. The gateway was built using the ESP32 module, which is a microcontroller module that uses a Wi-Fi communication feature and can directly connect to the Internet to forward the recorded data to the data center using the MQTT protocol with the publish-subscribe method. Communication testing of the LoRa devices was conducted in coastal areas where there were no barriers (free space). Analysis was conducted to determine the effect of the transmission distance on the percentage of packet loss and received signal strength indicator (RSSI).

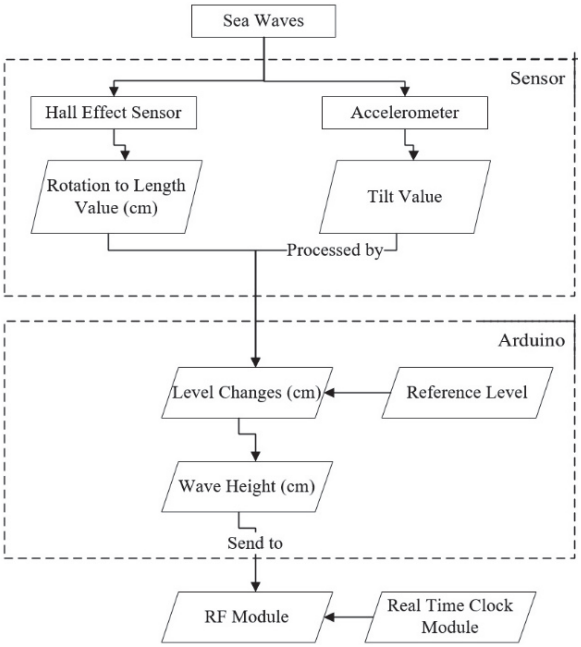

Fig. 8. Design development of wave height monitoring.

2.5. Instrument Evaluation

To evaluate the feasibility of the developed wave sensor, a series of tests were performed to determine its accuracy and consistency. As this research aims to build a tool with a new approach for capturing wave motion, it has a mechanical system that follows the movement of the water surface. A test platform was built using this mechanical model, in which the wave sensor was subjected to different conditions. In addition, this mechanical model provided information on the response of the sensor and its value under different wave conditions.

As previously explained, this tool is made using simple materials and is resistant to corrosion caused by seawater. It utilizes a rotation system to measure the height of waves. The rotation system uses four magnets attached to a freewheel holder, which trigger a Hall-effect sensor to read the position of the freewheel rotation. The number of turns was converted into distance, which is the change in sea level, as described in Eqs. (3) and (4).

As shown in **Fig. 8**, this tool uses an accelerometer sensor to generate acceleration value data that work on the device, and the output data from the accelerometer are required for further processing to obtain the desired value. The value of interest in wave-monitoring systems is the wave height. However, in this system, an accelerometer sensor is used to detect the slope of the tool caused by the impetus of ocean currents or ocean waves themselves.

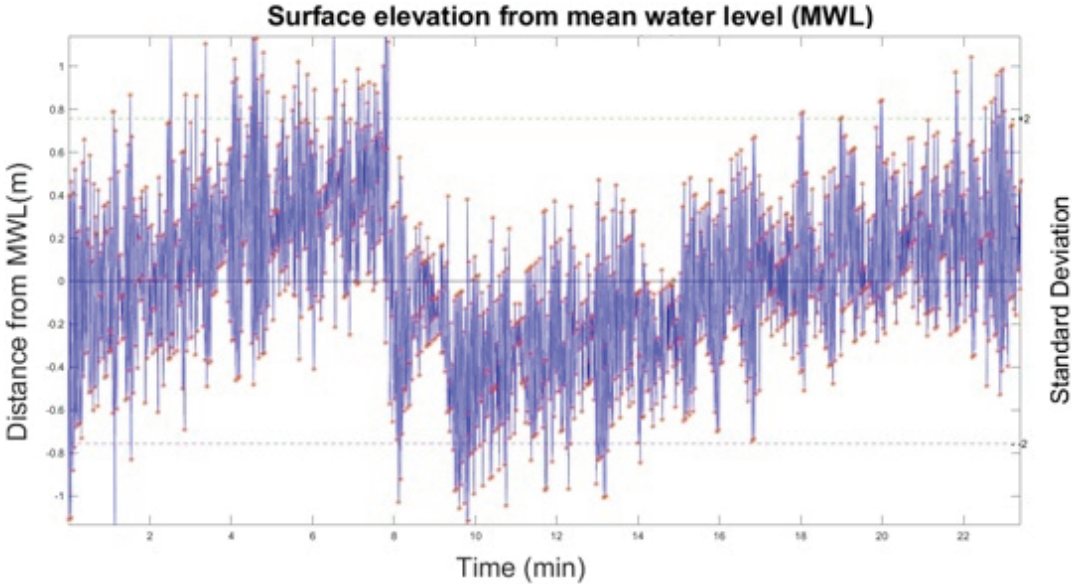

Fig. 9. Measured data from our instrument.

The results of the wave height reading were sent via the HopeRF-RFM9x radio module to the gateway installed on the mainland, to be sent to the server.

It was compared with wave height readings using ultrasonic sensors placed in the same location to evaluate the accuracy and consistency. The ultrasonic sensor uses a transmitter to send sound waves that are reflected when they hit the water surface, and the waves are captured by the receiver again.

Ultrasonic sensors are highly vulnerable to changes in sea-surface temperature and humidity [29, 30]. The ultrasonic sensor was placed on a sturdy pole and planted on the seabed to prevent movement when exposed to wind, waves, and ocean currents. The ultrasonic sensor was placed in a parallel position 10 m from the buoy instrument.

The measurement of the wave height between the tool and the wave height using an ultrasonic sensor with the amount of data (N) was statistically analyzed based on the root mean square error ($RMSE$) and the value of the correlation coefficient (R), where the value is determined by the following equation:

$$RMSE = \sqrt{\frac{1}{N}\sum_{i=1}^{N}(h_u - h_i)^2}, \quad \ldots\ldots\ldots \quad (8)$$

$$R^2 = \frac{\sum h_u h_i}{\sqrt{\sum h_u^2 \sum h_i^2}}. \quad \ldots\ldots\ldots \quad (9)$$

3. Result and Discussion

Instrument testing was conducted by placing the instrument in the sea at a certain depth based on the distance between the LoRa device and the shoreline. The study site had relatively calm sea waves with wave heights significantly below 2 m, which was suitable for placing the instrument for further testing.

The ability of the wave sensor to capture the actual motion of ocean waves was tested in a field. For field application, the wave sensor was placed approximately 50 m away from the beach. In this study, there are two categories of data retrieval processes: the first measurement data are only stored on the microSD without any data being sent to the mainland via the radio communication module, and the second for the system as a whole, namely, the data are sent via the radio communication module to the mainland. The purpose of this scenario is to determine the overall system performance.

In the first category of data stored in the microSD, 47,981 data points were recorded for approximately 2 h 20 min of testing duration. The test data for the tool obtained while reading the wave height are plotted in **Fig. 9**. The wave heights detected at the test locations varied over time. This indicates that the resulting wave conditions reflect a decrease in sea level (low tide) at that location.

Based on the measurement data shown in **Fig. 9**, it can be observed that the built instrument can read changes in the wave height well. The detected wave heights ranged from 0 cm to 18 cm. The combination of the accelerometer and Hall-effect sensors can record the height of the waves and adjust to changes in the slope of the tool when pushed by waves, wind, or ocean currents. From the obtained data, the slope of the instrument read by the accelerometer sensor during testing varies between 10°–35°.

However, to validate the accuracy of the instrument, it was necessary to compare it with ultrasonic sensors at the same location and time. Therefore, appropriate time adjustment must be conducted so that a comparison of the two values can be analyzed further. A comparison of the two datasets is shown in **Fig. 10**. As observed, the instru-

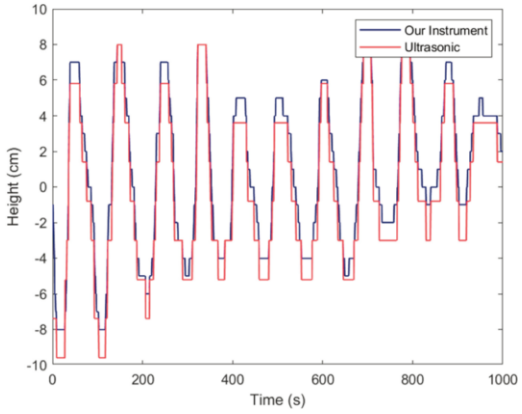

Fig. 10. Wave measurement comparison of our instrument to an ultrasonic sensor.

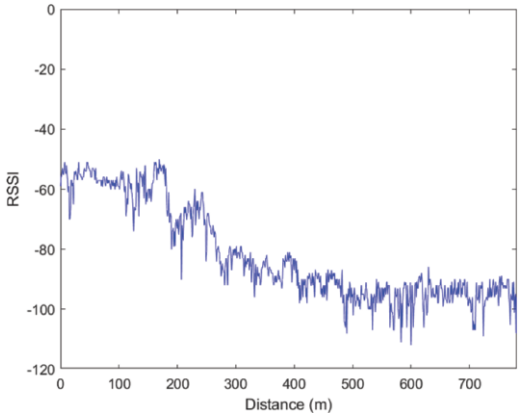

Fig. 12. RSSI signal based on distance.

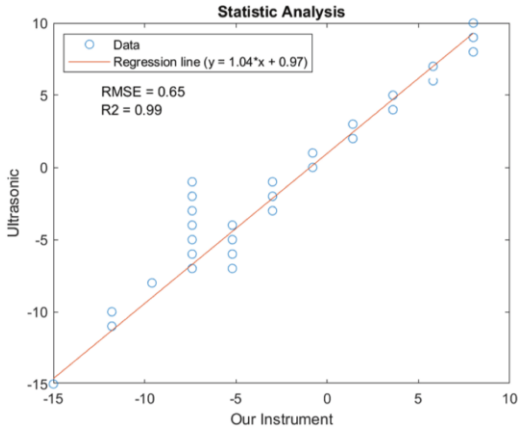

Fig. 11. Scatter plot of measured wave of our instrument compared to an ultrasonic sensor.

ments had different readings.

The difference in the wave height readings with the built instrument tended to be greater at the peak of the wave, whereas when the water level decreased, the wave valley of the ultrasonic sensor was lower. This could be due to the thrust of the waves, which caused the buoy to be thrown slightly away from the surface of the water because the buoy design was too light. **Fig. 10** also shows that the width and number of waves are relatively the same, although some data indicate that the instrument was built to produce more waves.

Furthermore, a statistical analysis, as illustrated in **Fig. 11**, was conducted to calculate the estimated wave-reading error of the developed instrument. To validate the results of the wave height measurements, the first step was to calculate the correlation value between the readings obtained using our instrument and those obtained using an ultrasonic sensor. The correlations determined using the R-squared method and Eqs. (8) and (9) yielded a coefficient of 0.99 in this case. This indicates that the measurements of our instrument were closely aligned with those of the ultrasonic sensor. Based on RMSE calculations, our instrument had an RMSE value of 0.65. This relatively small value implies that the reading model of our instrument is highly accurate in estimating wave heights compared with the readings obtained from the ultrasonic sensor.

Figure 12 shows the reliability of communication when sending data from the buoy to the mainland. The measurement results obtained by our instrument are sent to the gateway on the mainland using radio communication. RSSI and packet loss tests were conducted to measure the quality of data transfer from the sensor node to the gateway. The gateway was placed at an altitude of 1.5 m above ground level to maximize its ability to receive and send data. The RSSI value obtained from the LoRa HopeRF-RFM9x module ranged from −127 dBm to 0 dBm. The closer the value is to 0, the better is the signal. Packet loss is the number of packets that fail to reach the gateway during the travel of data. However, packets were not sent again if they failed to reach the gateway.

Based on the results, further distance can influence signal quality and packet loss, effecting LoRa reliability. Sea-level changes may affect the signal quality as the antenna continues to move owing to buoy motion. During sea trials, the instrument successfully measured the wave height and sent data to a gateway placed on land. The test results showed that the instrument system functioned and successfully recorded data by sampling every 100 ms at a distance of less than 500 m.

The collected data were then processed using the Wafo MATLAB toolbox to obtain the ocean wave characteristics at the test location. In addition, the mean water level (MWL) declined continuously from the beginning to the end of the test, where the MWL declined up to 3.2 cm in the first 20 min. This suggests that the developed instruments can adapt to MWL changes and hence can be used to measure tides.

As previously described, this research aimed to measure the characteristics of waves; therefore, a validation test was performed to investigate the mechanical and measurement system workability of the instrument. A validation test for the measurement system was conducted by analyzing the data to ensure that it worked accordingly. In this study, the data were analyzed using the Rayleigh approach with the Wafo Toolbox [33] to determine the wave

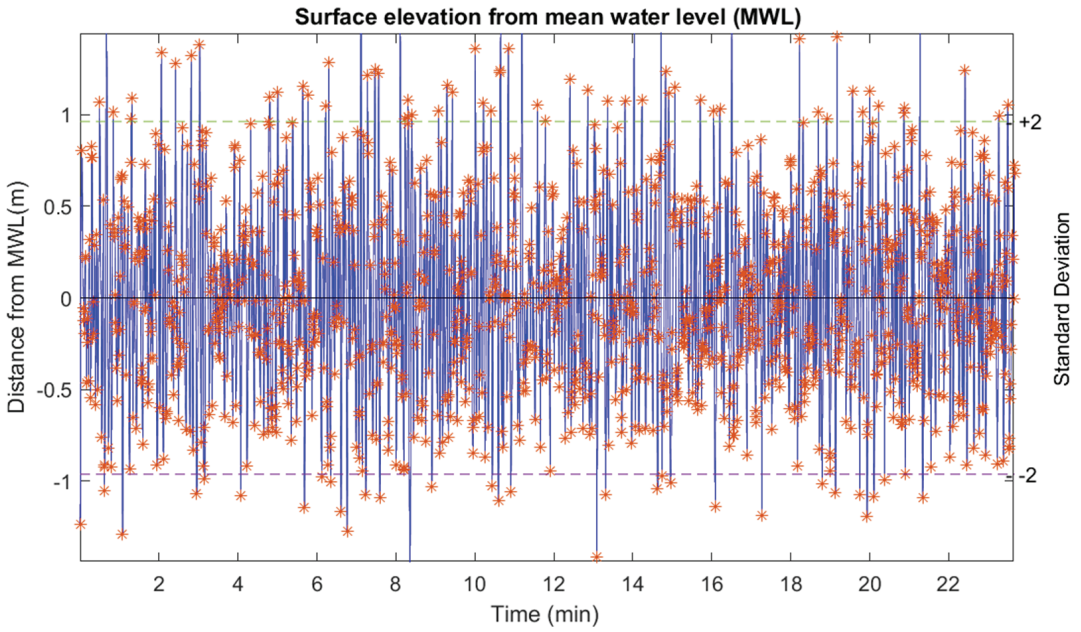

Fig. 13. Data stationarization.

crest height. This model is the simplest and most often used to determine the crests of waves.

As shown in **Fig. 9**, the data trend obtained by MWL changed and tended to decrease because of seawater tides. Therefore, to obtain the height parameters and characteristics of ocean waves, the data were stationarized by changing the MWL value at point 0, as shown in **Fig. 13**, after which the instrument value above 0 was the crest, and the position displacement below 0 was the trough of the wave. The detrend() function in the Wafo Toolbox was used for this process.

The analysis showed that the significant wave height (H_{m_0}) was 17.338 cm, the mean wave period (T_m) was 2.5880 s, and the peak period (T_p) was 2.9228 s. The highest significant wave height occurs between 8–16 minutes, as shown in **Fig. 14**. This follows the conditions of the seawaters of the test site, which have characteristics of the topographical conditions of the seabed that is sloping and has relatively small waves. However, the challenges of implementing the instrument over a more extended period will impact the material durability and instrument accuracy; hence, a different study focusing on the forces acting on the device should be performed.

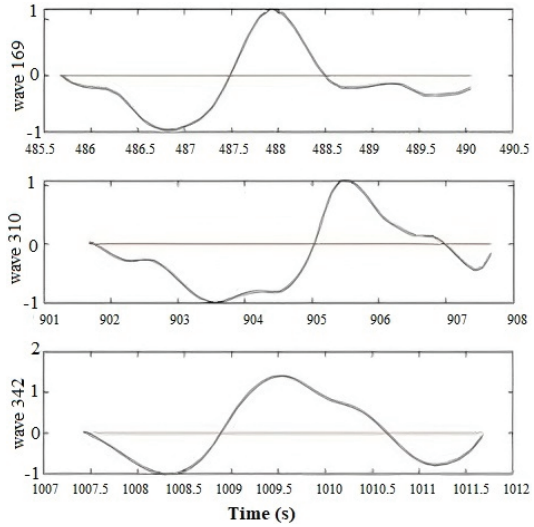

Fig. 14. Wave analysis.

4. Conclusion

This paper presents a novel instrument developed to address the insufficiency of marine monitoring instruments in Indonesia. The instrument utilizes a Hall-effect sensor in conjunction with an accelerometer to accurately measure the wave height, even when the instrument is not perpendicular to the surface of the water. The results indicate that the instrument achieves a satisfactory level of accuracy in reading wave height compared to the ultrasonic sensor, as evidenced by an RMSE value of 0.65 and an R^2 value of 0.99.

The integration of the accelerometer sensor enhances the ability of the instrument to adapt to slopes induced by waves, wind, and ocean currents, thereby improving its wave height detection capabilities. Communication between the buoy and the mainland through the radio module is effective within a distance of less than 500 m, but data loss becomes significant beyond that range.

An analysis of the wave characteristics at the test location demonstrated that the instrument could detect a maximum wave height of 17.338 cm and a peak period of 2.9228 s. Furthermore, the instrument adapted to changes in water levels during low tide. However, further tests un-

der extreme water conditions must be conducted to assess its robustness. In addition, considering its dimensions, the instrument appears suitable for deployment in shallow water.

Overall, this study offers a promising solution for addressing the limitations of marine monitoring instruments in Indonesia. The ability of the instrument to accurately measure the wave height, adapt to varying conditions, and potentially be applicable to shallow water makes it a valuable contribution to the field. Future research should focus on conducting comprehensive tests under extreme water conditions to validate their performance and evaluate their reliability in different marine environments.

Acknowledgments

The authors acknowledge the Directorate of Research and Community Service, the Directorate General of Research and Development of the Indonesian Ministry of Research, Technology, and Higher Education, and the Polytechnic State of Banyuwangi for their support.

References:

[1] L. H. Holthuijsen, "Waves in Oceanic and Coastal Waters," Cambridge University Press, 2007. https://doi.org/10.1017/CBO9780511618536

[2] C. R. Nichols and R. G. Williams, "Encyclopedia of Marine Science," Viva-Facts On File, 2009.

[3] E. S. Haq, D. Suwardiyanto, M. D. Ayatullah, E. M. Rini, H. Sutiksno, and E. Setyati, "The Coastal Early Warning System Based on Buoy Sensor Measurement," 2019 2nd Int. Conf. of Computer and Informatics Engineering (IC2IE), pp. 39-43, 2019. https://doi.org/10.1109/IC2IE47452.2019.8940821

[4] K.-H. Kim, B.-S. Shin, and K.-T. Shim, "Investigation of Coastal Environment Change Using Wave Measurement Sensors and Geographical Laser Scanner," J. of Sensors, Vol.2019, Article No.e3754972, 2019. https://doi.org/10.1155/2019/3754972

[5] S. A. Subiyanto, M. L. Syamsudin, and I. Faizal, "Instrumentation System for Coastal Wave Parameter Monitoring Based on Telemetry Technology Using Accelerometer," World Science News, Vol.148, pp. 72-89, 2020.

[6] J. Wang, L. Aouf, X. Wang, B. Li, and J. Wang, "Remote Cross-Calibration of Wave Buoys Based on Significant Wave Height Observations of Altimeters in the Northern Hemisphere," Remote Sens., Vol.12, Issue 20, pp. 1-12, 2020. https://doi.org/10.3390/rs12203447

[7] J. Beck, O. Wannick, and H. Bremerhaven, "Wave Measuring Buoy," Forsch! – Studentisches Online-Journal der Univ Oldenbg, pp. 61-74, 2017.

[8] K. Kobune, H. Sasaki, and N. Hashimoto, "Characteristics of Ocean Waves Off Cape Nojima in the Northwestern Pacific, Measured With a Discus Buoy," Ministry of Transport, Nagase Yokosuka Japan, "Report of the Port and Harbour Ressearch Institute," Vol.24, No.3, pp. 3-30, 1985.

[9] N. K. Kumar, R. Savitha, and A. A. Mamun, "Ocean Wave Characteristics Prediction and Its Load Estimation on Marine Structures: A Transfer Learning Approach," Marine Structures, Vol.61, pp. 202-219, 2018. https://doi.org/10.1016/j.marstruc.2018.05.007

[10] G. Joodaki, H. Nahavandchi, and K. Cheng, "Ocean Wave Measurement Using GPS Buoys," J. Geodetic Science, Vol.3, Issue 3, pp. 163-172, 2013. https://doi.org/10.2478/jogs-2013-0023 https://doi.org/10.2478/jogs-2013-0023

[11] K. Raghukumar, G. Chang, F. Spada, C. Jones, and T. Jannsen, "Directional Spectrum Measurements by the Spotter: A New Developed Wave Buoy," Ocean Waves Work, Session 2, 2019.

[12] A. V. Babanin, P. P. Verkeev, B. B. Krivinsky, and V. G. Proshchenko, "Measurement of Wind Waves by Means of a Buoy Accelerometer Wave Gauge," Physical Oceanography, Vol.4, No.5 pp. 399-407, 1993. https://doi.org/10.1007/BF02198503

[13] D. Bajpai, U. Porov, G. Srivastav, and N. Sachan, "Two Way Wireless Data Communication and American Sign Language Translator Glove for Images Text and Speech Display on Mobile Phone," 2015 5th Int. Conf. on Communication Systems and Network Technologies, pp. 578-585, 2015. https://doi.org/10.1109/CSNT.2015.121

[14] Y. Y. Yurovsky and V. A. Dulov, "Compact Low-cost Arduino-based Buoy for Sea Surface Wave Measurements," 2017 Progress in Electromagnetics Research Symp. - Fall (PIERS-FALL), pp. 2315-2322, 2017. https://doi.org/10.1109/PIERS-FALL.2017.8293523

[15] K. H. Christensen, J. Röhrs, B. Ward, I. Fer, G. Broström, Ø. Saetra, and Ø. Breivik, "Surface Wave Measurements Using a Ship-Mounted Ultrasonic Altimeter," Methods in Oceanography, Vol.6, pp. 1-15, 2013. http://dx.doi.org/10.1016/j.mio.2013.07.002

[16] M. J. Allis, W. L. Peirson, and M. L. Banner, "Application of LiDAR As a Measurement Tool for Waves," The 21st Int. Offshore and Polar Engineering Conf., pp. 373-379, 2011.

[17] K. Martins, C. E. Blenkinsopp, and J. Zang, "Monitoring Individual Wave Characteristics in the Inner Surf With a 2-Dimensional Laser Scanner (LiDAR)," J. Sensors, Vol.2016, Article No.e7965431, 2016. https://doi.org/10.1155/2016/7965431

[18] T. P. Lyman, K. Elsmore, B. Gaylord, J. E. K. Byrnes, and L. P. Miller, "Open Wave Height Logger: An Open Source Pressure Sensor Data Logger for Wave Measurement," Limnology and Oceanography Methods, Vol.18, Issue 7, pp. 335-345, 2020. https://doi.org/10.1002/lom3.10370

[19] I. Alifdini, A. Darari, and D. N. Sugianto, "Identification of Ocean Wave Measurement in Sungai Suci Beach by Using Drone and Ultrasonic Sensor," J. of Engineering and Applied Sciences, Vol.13, Issue 21, pp. 8973-8980, 2018.

[20] M. C. Marimon, G. Tangonan, N. J. Libatique, and K. Sugimoto, "Development and Evaluation of Wave Sensor Nodes for Ocean Wave Monitoring," IEEE Systems J., Vol.9, Issue 1, pp. 292-302, 2015. https://doi.org/10.1109/JSYST.2013.2284102

[21] S. Prajapati and R. Parab, "Design of Digital Tachometers Based on Different Sensing Techniques," Int. J. of Computer Science Engineering., Vol.7, Issue 11, pp. 73-78, 2019. https://doi.org/10.26438/ijcse/v7i11.7378

[22] K. Nakano, T. Takahashi, and S. Kawahito, "Angle Detection Methods for a CMOS Smart Rotary Encoder," J. Robot. Mechatron., Vol.17, No.4, pp. 469-474, 2005. https://doi.org/10.20965/jrm.2005.p0469

[23] T. Masuda and M. Kajitani, "High Accuracy Calibration System for Angular Encoders," J. Robot. Mechatron., Vol.5, No.5, pp. 448-452, 1993. https://doi.org/10.20965/jrm.1993.p0448

[24] İ. Yariçi and Y. Öztürk, "A New Approach to Linear Displacement Measurements Based on Hall Effect Sensors," Turkish J.of Electrical Engineering and Computer Sciences, Vol.31, No.1, pp. 238-248, 2023. https://doi.org/10.55730/1300-0632.3981

[25] B. Zhou and C. Huang, "Magnetic Poles Position Detection of Permanent Magnet Linear Synchronous Motor Using Four Linear Hall Effect Sensors," Actuators, Vol.12, Issue 7, Article No.269, 2023. https://doi.org/10.3390/act12070269

[26] H. Tanaka, A. Nakata, and H. Ide, "Study of Motion Monitoring Using an Accelerometer – Unrestrained Measurement –," J. Robot. Mechatron., Vol.11, No.2, pp. 148-152, 1999. https://doi.org/10.20965/jrm.1999.p0148

[27] B. Meng, Y. Wang, W. Sun, and X. Yuan, "A Novel Diagnosis Method for a Hall Plates-Based Rotary Encoder with a Magnetic Concentrator," Sensors, Vol.14, Issue 8, pp. 13980-13998, 2014. https://doi.org/10.3390/s140813980

[28] H. Kimura, M. Nakamura, N. Inou, M. Matsudaira, and M. Yoshida, "Identification Method of Sensor Directions and Sensitivities in Multi-Axis Accelerometer (Actual Measurement of Direction Tensor and Sensitivity Tensor)," Trans. of the Japan Society of Mechanical Engineers, Vol.78, Issue 786, pp. 499-507, 2012. https://doi.org/10.1299/kikaic.78.499

[29] A. Rocchi, E. Santecchia, F. Ciciulla, P. Mengucci, and G. Barucca, "Characterization and Optimization of Level Measurement by an Ultrasonic Sensor System," IEEE Sensors J., Vol.19, Issue 8, pp. 3077-3084, 2019. https://doi.org/10.1109/JSEN.2018.2890568

[30] M. I. Bello, S. M. Gana, M. I. Faruk, and M. J. Umar, "Autonomous Ultrasonic Based Water Level Detection and Control System," Nigerian J. of Technology, Vol.37, No.2, pp. 508-513, 2018. https://doi.org/10.4314/njt.v37i2.29

[31] H. Hanan, A. A. N. Gunawan, and M. Sumadiyasa, "Water Level Detection System Based on Ultrasonic Sensors HC-SR04 and Esp8266-12 Modules with Telegram and Buzzer Communication Media," Instrumentation Mesure Métrologie, Vol.18, Issue 3, pp. 305-309, 2019. https://doi.org/10.18280/i2m.180311

[32] M. Cattani, C. A. Boano, and K. Römer, "An Experimental Evaluation of the Reliability of Lora Long-Range Low-Power Wireless Communication," J. of Sensor and Actuator Networks, Vol.6, Issue 2, 2017. https://doi.org/10.3390/jsan6020007

[33] P. A. Brodtkorb, P. Johannesson, G. Lindgren, I. Rychlik, J. Ryden, and E. Sjo, "WAFO – A Matlab Toolbox for Analysis of Random Waves and Loads," The 10th Int. Offshore and Polar Engineering Conf. 2000, pp. 343-350, 2000.

Name:
Devit Suwardiyanto

ORCID:
0000-0003-2282-4273

Affiliation:
Department of Informatics Engineering, Politeknik Negeri Banyuwangi

Address:
Jalan Raya Jember KM-13 Labanasem, Kabat, Banyuwangi 68461, Indonesia

Brief Biographical History:
2009- Lecturer, Politeknik Negeri Banyuwangi

Main Works:
• "A Novel Multi-Patient Mechanical Ventilator Drive System Using Continuously Variable Transmission and Reverse Gearbox," Int. J. on Advanced Science, Engineering and Information Technology, Vol.11, No.6, pp. 2293-2298, 2021.

Membership in Academic Societies:
• International Assosiation of Engineers (IAENG)

Name:
Endi Sailul Haq

ORCID:
0000-0002-7501-3100

Affiliation:
Department of Computer Engineering, Politeknik Negeri Banyuwangi

Address:
Jalan Raya Jember KM-13 Labanasem, Kabat, Banyuwangi 68461, Indonesia

Brief Biographical History:
2010- Lecturer, Politeknik Negeri Banyuwangi
2021- Head of Research and Community Service, Politeknik Negeri Banyuwangi

Main Works:
• "A Novel Multi-Patient Mechanical Ventilator Drive System Using Continuously Variable Transmission and Reverse Gearbox," Int. J. on Advanced Science, Engineering and Information Technology, Vol.11, No.6, pp. 2293-2298, 2021.

Membership in Academic Societies:
• Indonesian Society of Applied Science (ISAS)

Name:
Mohamad Dimyati Ayatullah

ORCID:
0000-0002-7214-6733

Affiliation:
Department of Bussines and Informatics, Politeknik Negeri Banyuwangi

Address:
Jalan Raya Jember KM-13 Labanasem, Kabat, Banyuwangi 68461, Indonesia

Brief Biographical History:
2013- Lecturer, Politeknik Negeri Banyuwangi

Main Works:
• "The Coastal Early Warning System Based on Buoy Sensor Measurement," 2019 2nd Int. Conf. of Computer and Informatics Engineering (IC2IE), pp. 39-43, 2019.
• "The Internet-of-Things-based Water Monitoring and Billing System using Lora and Remotely-Controlled Water Valve," 2022 6th Int. Conf. on Information Technology, Information Systems and Electrical Engineering (ICITISEE), 2022.

Name:
Bayu Rudiyanto

ORCID:
0000-0002-4708-629X

Affiliation:
Associate Professor, Department of Renewable Energy Engineering, Politeknik Negeri Jember

Address:
Jalan Mastrip No.164, Krajan Timur, Jember 68121, Indonesia

Brief Biographical History:
2002- Lecturer, Politeknik Negeri Jember
2011- Visiting Scientist, Chung Yuan Christian University

Main Works:
• "A Genetic Algorithm Approach for Optimization of Geothermal Power Plant Production: Case Studies of Direct Steam Cycle in Kamojang," South African J. of Chemical Engineering, Vol.45, pp. 1-9, 2023.

Membership in Academic Societies:
• The Institute of Engineers Indonesia (PII)
• Frontier in Thermal Engineering